Trans Indian Inst Met (2022) 75(8):2169–2177
https://doi.org/10.1007/s12666-022-02598-2

ORIGINAL ARTICLE

Influence of Nitrogen on Grain Size-Dependent Sensitisation and Corrosion Resistance of 316L (N) Austenitic Stainless Steels

S. Aamani[1] · C. R. Das[2,3] · Surendra K. Martha[4] · S. K. Albert[2,3] · Bharat B. Panigrahi[1]

Received: 17 September 2021 / Accepted: 17 March 2022 / Published online: 11 April 2022

Abstract Influences of grain size and low energy Σ boundaries on intergranular corrosion (IGC) resistance of low and high nitrogen containing 316L austenitic stainless steel (ASS) have been investigated in this study after solutionising and sensitisation heat treatments. With increase in solutionising temperature, an increase in average grain size with a larger distribution (larger standard deviation) was also observed. Variation of grain size was larger in the low nitrogen containing ASS as compared to that of high nitrogen containing ASS. Full width half maximum (FWHM) was observed to increase with increasing solutionising temperature and grain size in both the steels. However, relatively finer grains accompanied by higher FWHM were observed in high nitrogen containing ASS. The IGC resistance of solutionised and sensitised steels was studied using double-loop electrochemical potentiokinetic reactivation (DL-EPR) method. It was observed that the degree of sensitisation (DOS) had reduced significantly in high nitrogen containing ASS after sensitisation heat treatments. Improved IGC resistance of steel with increased nitrogen content could be attributed to the increased fraction of low energy Σ boundaries.

✉ C. R. Das
chitta@igcar.gov.in

✉ Bharat B. Panigrahi
bharat@msme.iith.ac.in

[1] Department of Materials Science and Metallurgical Engineering, Indian Institute of Technology Hyderabad, Kandi, Sangareddy, Telangana 502285, India

[2] Indira Gandhi Centre for Atomic Research, Kalpakkam, India

[3] Homi Bhabha National Institute, Kalpakkam, India

[4] Department of Chemistry, Indian Institute of Technology Hyderabad, Kandi, Sangareddy, Telangana 502285, India

Keywords Austenitic stainless steel · Solutionisation · Corrosion · Grain size · Sigma boundaries and Degree of sensitisation

1 Introduction

Grain size (GS) plays an important role in improving the strength and corrosion resistance of ASS. Corrosion resistance of iron-based alloys was reported to increase with increasing GS. Taiwad et al. [1] reported a significant improvement in the corrosion resistance of Cr-Mn stainless steels with increasing GS. Similar results were reported in Ni-base superalloys by Kaithwas et al. [2] and in AISI 316L(N) stainless steels (SS) containing 0.0561 and 0.0716 wt% N by Parvathavarthini et al. [3]. This was attributed to the delay in $M_{23}C_6$ precipitates at the grain boundaries during sensitisation.

Generally, mechanical properties of stainless steel or single phase alloys vary inversely with the GS [4, 5]. Similarly, attempts were made to establish a relationship between GS and corrosion resistance of annealed and sensitised steels [2, 4, and 5]. In those studies, GS was varied from 39–135, 20–180 and 50–250 µm [1–3]. In industrial practice, smaller GS is commonly preferred, but presence of mixed size grains, i.e. small grains and relatively larger grains, were reported in forged AISI 304 L SS [6]. Saju et al. [7] reported a correlation between degree of sensitisation (DOS) and GS in 304 L SS using NDT (non-destructive testing) technique. Kaithwas et al. [2] reported the presence of finer grains along with coarser grains in nickel base alloy, which introduces a scatter in DOS values. Therefore, it is important to understand not only the influence of GS, but also its distribution (standard

deviation, SD) on the corrosion resistance of ASS. Corrosion resistance of stainless steel deteriorates if it experiences heating or cooling cycles during welding or heat treatment. Chromium-rich $M_{23}C_6$ precipitation occurs at the grain boundary during this exposure, causing loss of corrosion resistance which is known as sensitisation [3].

The effect of GS on sensitisation behaviour of AISI 304L SS and AISI 316 SS was reported in the literature; however, there are very few papers that discuss the effect of GS in low and high nitrogen containing AISI 316L stainless steels. ASS has very good uniform corrosion resistance [8]. But prone to localised corrosion such as intergranular corrosion (IGC), inter-granular stress corrosion and pitting corrosion. Nitrogen commonly improves the pitting corrosion resistance of steel [9]. Poonguzhali et al. [10] reported an improvement in the pitting corrosion resistance of AISI 316L SS with increasing nitrogen content from 0.07 to 0.22 wt%; however, corrosion resistance was reported to be reduced in the sensitised condition. Anita et al. [11] reported an improvement in the stress corrosion cracking (SCC) resistance with increasing nitrogen content up to 0.14 wt% in AISI 316L SS. But, SCC resistance was reported to be inferior when nitrogen content was increased to 0.22 wt%. This anomaly of corrosion behaviour at higher nitrogen containing ASS needs attention. Stainless steel when exposed to a temperature range of 450 to 850 °C during heat treatment or welding, chromium-rich $M_{23}C_6$ carbide precipitates at the grain boundaries. This process adversely affects the passive film formation during corrosion at the grain boundaries due to reduced chromium content locally below 12 wt% [12].

One common approach to improve the corrosion resistance of this class of low stacking fault energy materials is to increase the population of low energy coincidence lattice site (CSL, also known as Σ boundaries) boundaries by employing grain boundary engineering [13–15]. Tsurekawa et al. [13] and Michiuchi et al. [14] have shown that 304 and 316 ASS having 60 to 70% Σ boundaries are less prone to IGC. Schino and Kenny [16] reported that the general corrosion resistance of nitrogen containing (0.37 wt%) AISI 304 ASS was decreased with grain refinement, whereas IGC resistance and pitting corrosion resistance were increased with decreasing GS in the sensitised condition. The effect of GS on corrosion resistance seems to be inconsistent in the literature [1–3, 16]. This is possibly due to the differences in the processing history of the steel, i.e. use of thermomechanical processing prior to recrystallisation heat treatment and heat treatment alone to obtain different GS. GS obtained by different means will yield different stored energies in the microstructure and hence exhibits different corrosion behaviour.

With increasing demand for improved corrosion resistance, creep and fatigue resistance, nitrogen containing 316L SS is in great demand. Though there are numerous reports on influence of GS on IGC, reports on influence of nitrogen and GS variations on IGC are limited. High nitrogen (0.144 wt%) containing AISI 316L SS is being considered for Fast Breeder Reactor (FBR) application in India to enhance the reactor life [17]. However, corrosion resistance of this steel, particularly in the sensitised condition has not been clearly understood, which is the major motivation behind the present study. The objective of the present study is to understand the influence of GS and GS variations on IGC in low and high nitrogen containing AISI 316L SS.

2 Experimental

2.1 Heat Treatments

Low nitrogen and high nitrogen containing AISI 316LSS were received in the form of rectangular plates (∼ 12 mm thick) in the annealed condition (1100 °C/60 min). Chemical compositions (wt%) of low and high nitrogen containing AISI 316L SS are C:0.01, Mn:1.41, Si:0.41, Cr:17.84, Ni:12.43, Mo:2.16, S:0.006, P: 0.036, N:0.01, and Fe: bal and C:0.02, Mn:1.98, Si:0.48, Cr:17.61, Ni:10.46, Mo:2.34, N:0.144, S:0.01, P: 0.036 and Fe: bal, respectively. As-received steels were cut into small rectangular pieces for two different sets of heat treatments. Initially, solutionisation heat treatment was carried out at three different temperatures, i.e. at 1000, 1050 and 1100 °C for 60 min in a tubular furnace in argon atmosphere, followed by quenching in water. These set of specimens were designated as LN-ST and HN-ST for low and high nitrogen containing SS, respectively. Solutionised specimens were subjected to further heat treatment (called as sensitisation) at a relatively lower temperature of 675 °C for 60 min followed by water quenching. These specimens were designated as LN-ST-S and HN-ST-S for low and high nitrogen containing AISI 316L SS, respectively. The sensitisation temperature was chosen, based on the work of Momeni et al. [18].

2.2 Corrosion Test

Specimens obtained after various heat treatments, i.e. after solutionising and sensitisation, were cut into $8.0 \times 8.0 \times 3.0$ mm^3 and surfaces were polished using 1 μm diamond paste for the corrosion tests. Mould was prepared using brass ring and contact was made between the specimen and brass ring using silver paste and continuity between brass and specimen was confirmed using multimeter. An area of 0.64 cm^2 of the specimen surface was exposed, whereas remaining area was lacquered using

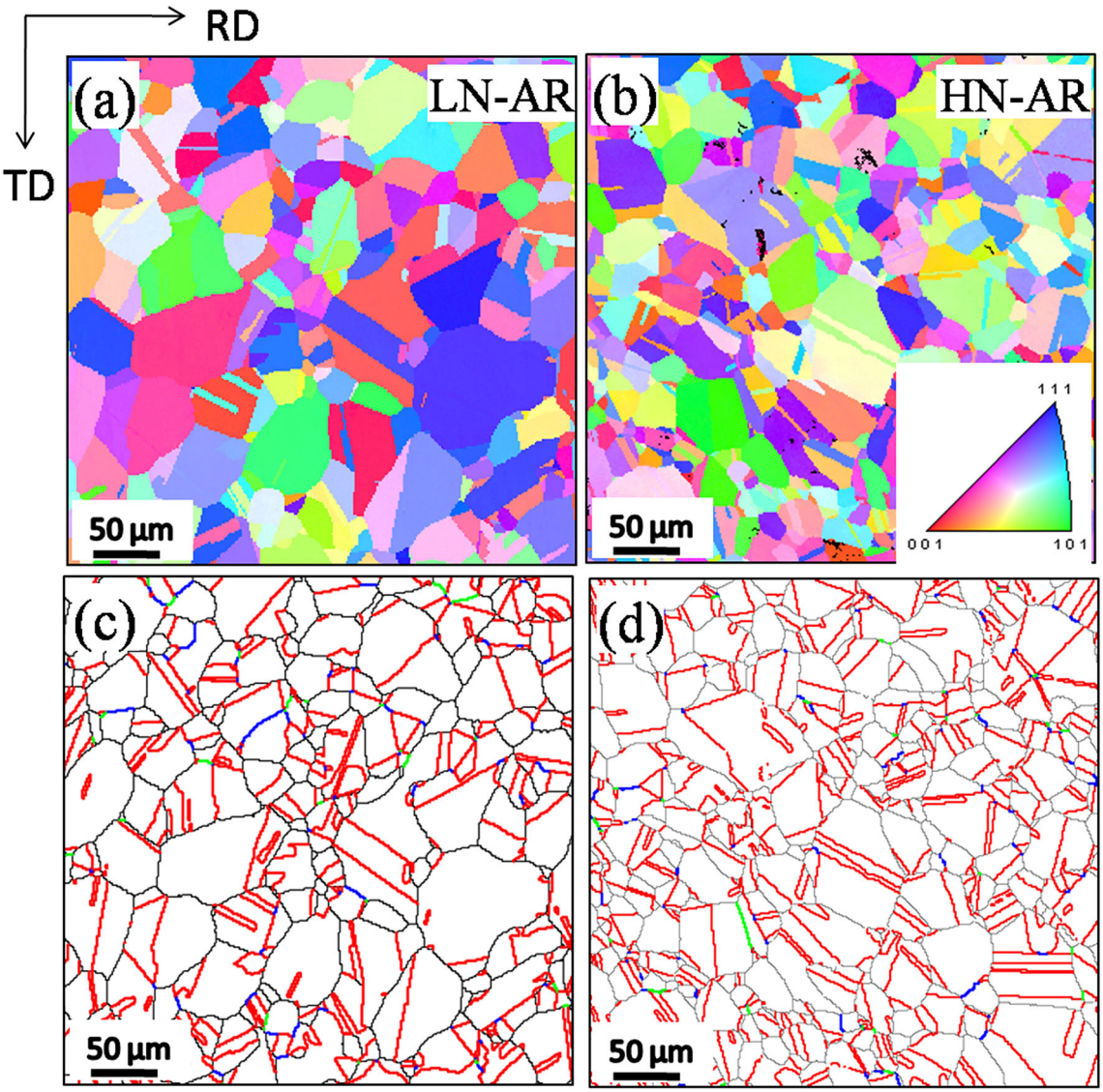

Fig. 1 IPF maps of as-received steels: **a** LN-ST and **b** HN-ST specimen; and respective OIM maps of **c** LN-ST and **d** HN-ST (colour code: Σ 3—red; Σ 9—blue; Σ 27—green; HAGB (high angle grain boundaries)—black)

enamel. Specimen was immersed in the test solution and open circuit potential (OCP) was recorded for 60 min to achieve stable potential. The corrosion tests were conducted using doubleloop electrochemical potentiokinetic reactivation (DL-EPR) technique in deaerated 0.5 M sulphuric acid and 0.01 M potassium thiocyanate (KSCN) solution at room temperature [19]. The medium for DL-EPR testing was chosen from the literature [20]. The concentration of both H_2SO_4 and KSCN was optimised based on sensitivity of etching, sensitivity to detect weak depleted zones at the boundaries and reproducibility of test responses [20]. Standard three electrode cell was used with a saturated calomel electrode (SCE) as reference electrode, platinum mesh as a counter electrode and the specimen as a working electrode. DL-EPR tests were performed at room temperature in the scan range of nearly −0.3 V to + 0.3 V SCE using a scan rate of 1.667 mV/s. Degree of sensitisation [DOS = $(I_r/I_a) \times 100$] [19–21] of both steels in different heat treatment conditions was evaluated using reactivation current (I_r) and activation current (I_a) and the measured DOS values were compared to understand their resistance against sensitisation.

2.3 Phases and Microstructure Characterisation

X-ray diffraction (XRD) analysis of both the steels at every stage of heat treatment was carried out using Malvern Panalytical X'PERT PRO XRD machine equipped with a Cu (K_α) target. Specimens were scanned using a step size of 0.0167°(2θ) and with an acquisition time of 1000 s at

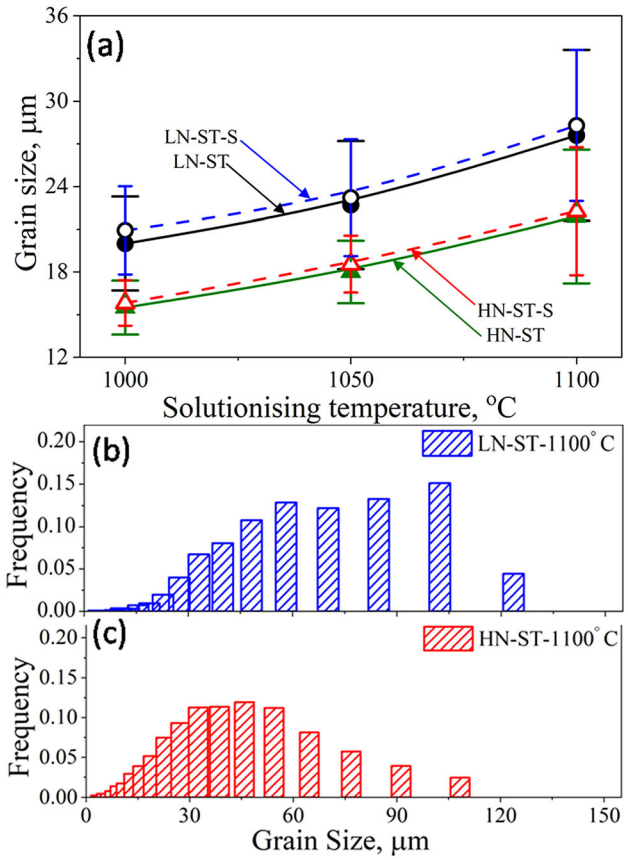

Fig. 2 **a** Variation of grain size as a function of solutionising temperature in solutionised and sensitised conditions. Frequency plots showing a variation of grain size after solutionising heat treatment at 1100 °C for: **b** LN-ST and **c** HN-ST specimen

each step. The specimens were polished using 1200 fine grit emery paper for XRD studies. Observed XRD peaks were analysed to measure the full width at half maximum (FWHM).

Specimens were polished metallographically till 1.0 µm diamond slurry. For the electron backscatter diffraction (EBSD) analysis, specimens were finally polished electrochemically in 10% perchloric acid + 90% methanol solution using standard procedure. EBSD studies were carried out using Carl-Zeiss make Supra 40 Field Emission Scanning Electron Microscope (FESEM) operating at 20 kV. EBSD scans were carried out for an area of 1200 × 1200 µm using the step size of 1.0 µm. The acquired EBSD data were analysed using the TSL-OIM^{TM} software (version 7) for the grain boundary character distribution (GBCD) characterisation. The grain boundary characters were defined by CSL model according to the Brandon criterion ($V_m = V_o \sum^{-1/2}$, where V_m is the maximum angular deviation and $V_o = 15°$) [22]. After the DL-EPR test, the scanned areas were studied through FESEM to analyse the corrosion attack on the microstructure.

3 Results and Discussion

3.1 Microstructural and Phase Analysis

Inverse pole figure (IPF) and orientation imaging microscopy (OIM) maps of as-received (AR) specimens are shown in Fig. 1a, b and c, d, respectively. The grain size is observed to be smaller in HN-ST specimen as compared to LN-ST specimen, as shown in Fig. 1a, b. GS of AR low and high nitrogen ASS are 18 and 14 µm, respectively. Fraction of twins appears to be higher in

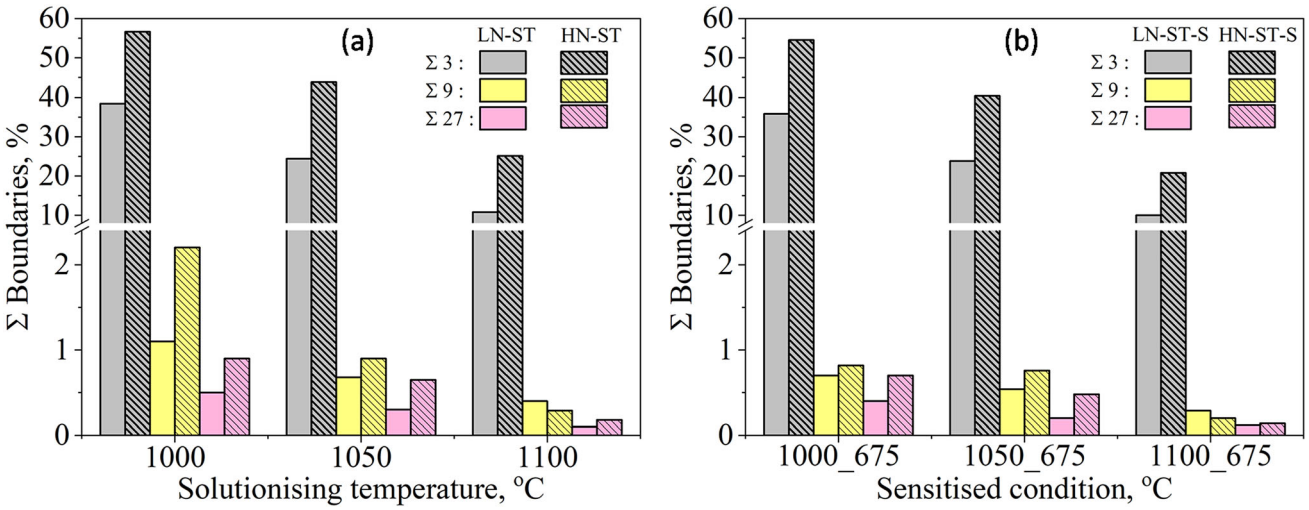

Fig. 3 **a** Variations of Σ boundaries as a function of solutionising temperature in low and high nitrogen containing ASS and **b** Variations of Σ boundaries as a function of solutionising temperature in low and high nitrogen containing ASS after sensitisation

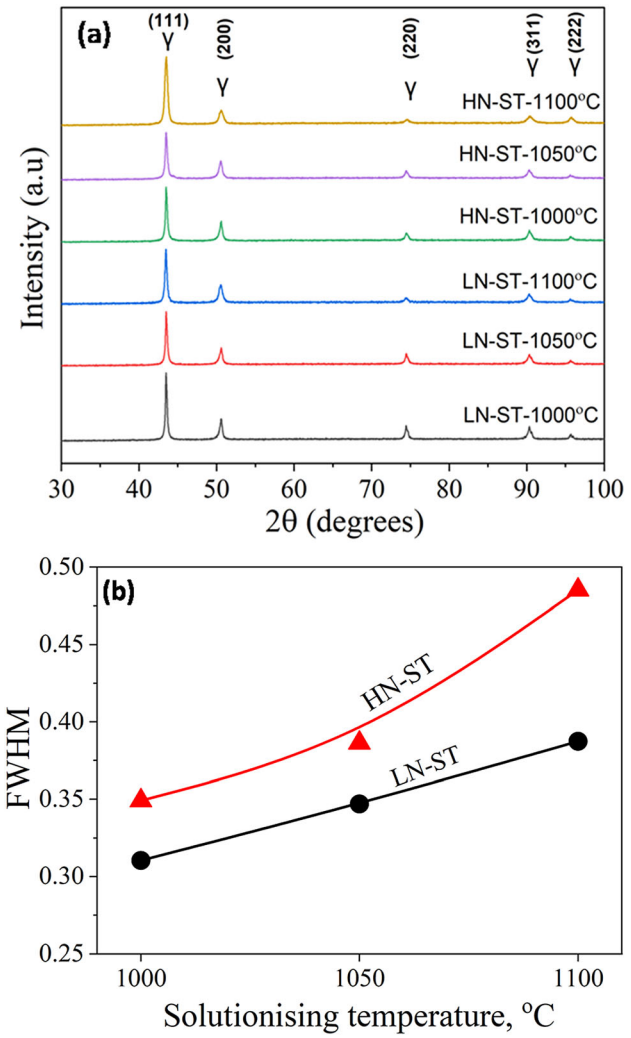

Fig. 4 **a** XRD diffractograms of solutionised low and high nitrogen containing ASS, at different temperatures, **b** Variation of FWHM values of (111) peak as a function of solutionising temperature

HN-ST specimen as compared to that of LN-ST specimen (Fig. 1c,d). The variation of GS as a function of solutionising temperature is shown in Fig. 2a for solutionised and sensitised conditions. It is observed that the GS remains smaller in HN-ST specimens as compared to LN-ST specimens in all conditions. There is no measureable change in GS after sensitisation, as shown in Fig. 2a. The scatter of GS is lower in HN-ST specimen as compared to LN-ST specimens, which could be seen in Fig. 2b and c for the specimen solutionised at 1100 °C. The standard deviation (SD) of the GS is more in LN-ST specimens, which increases with increasing solutionising temperature, as shown in Fig. 2a.

Figure 3a shows the fraction of Σ boundaries (i.e. Σ3, Σ9 and $\Sigma \leq 29$ boundaries) as a function of solutionising temperature. It is apparent that the fraction of Σ boundaries decreases gradually with increasing solutionising temperature in both the steels. Fraction of Σ3 boundary is significantly higher as compared to other Σ boundaries (i.e. Σ9 and $\Sigma \leq 29$) in HN-ST specimens compared to LN-ST. This difference in Σ3 boundaries between HN-ST and LN-ST specimen can be attributed to variation of stacking fault energies caused by nitrogen. Some researchers reported that nitrogen increases the stacking fault energy [23, 24], whereas other group reported that it reduces stacking fault energy [25, 26]. Yakubtsov et al. [23] calculated the stacking fault energy of ASS and have shown that it increases to a maximum value for 0.3 wt% nitrogen steel, and decreases when the nitrogen content is increased to 0.5 wt%. Aamani et at [27]. recently reported that ASS containing 0.144 wt% nitrogen produces higher CSL fraction as compared to ASS without nitrogen upon grain boundary engineering heat treatment. This observation is in agreement with the present finding i.e. HN-ST specimen has higher CSL as compared to LN-ST specimen. After sensitisation, fraction of low energy Σ boundaries remaines higher in HN-ST-S specimens as compared to LN-ST-S specimens, as shown in Fig. 3b. Fractions of Σ9 and Σ27 have reduced relatively more in HN-ST-S after sensitisation. Reduction in fraction of CSL at higher annealing temperature as compared to lower temperature can be attributed to the faster rate of grain boundary migration similar to that reported in Ti-modified ASS [28]. As grain boundary area is higher than the area of twin boundaries in coarse-grained material, it yields reduced Σ boundaries fraction [29]. Reduction of Σ9 and Σ27 boundary fractions in sensitised steels as compared to annealed steel, suggests reduced interaction of Σ3 boundaries as proposed by Randle [30]. In a coarser-grained material, the grain boundary migration is the most favoured way to reduce overall energy rather than formation of annealing twins. During faster grain growth at higher temperature, time may not be sufficient for nucleation of twins. Thus, reduction in the energy occurs through grain growth. This is in agreement with observation reported by Mandal et al. [28] in Ti-modified ASS. It may be worth mentioning that the total $\Sigma \leq 29$ boundary is higher in as-received material compared to other heat treatment conditions. Total CSL fraction in low and high nitrogen containing ASS is 47 and 68, respectively, which is comparable to that observed in respective steel after 1000 °C annealing. But Σ 3 fraction is marginally higher in 1000 °C condition compared to as-received steel.

XRD diffractograms of solutionised specimens show that all the peaks belong to austenite phase, as shown in Fig. 4a. It is expected that with increasing solutionising temperature, peaks get sharper due to annihilation of dislocations or reduction in dislocation density, but in the present case, the unusual peak broadening (i.e. increased FWHM) is observed with increasing solutionising

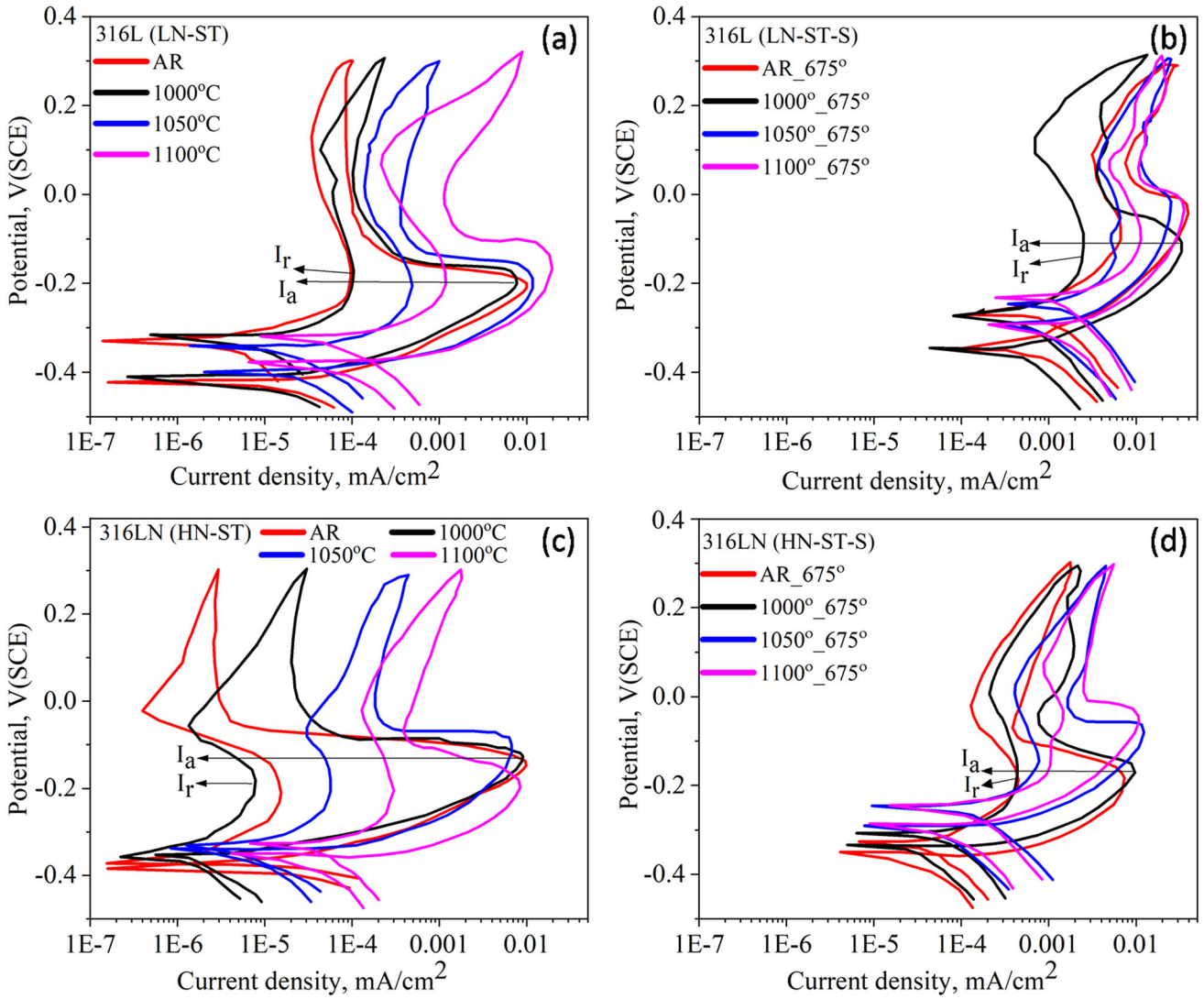

Fig. 5 DL-EPR plots obtained for solutionised and sensitised steels: **a** LN-ST specimens, **b** LN-ST-S specimens, **c** HN-ST specimens and **d** HN-ST-S specimens along with as-received specimens

temperature, as shown in Fig. 4b. This could be attributed to the evolution of a few smaller grains along with grain coarsening [2]. In spite of having higher FWHM, higher nitrogen containing ASS shows higher fraction of low energy Σ boundaries as compared to low nitrogen containing ASS as mentioned earlier.

3.2 Corrosion

Results of corrosion tests (i.e. DL-EPR plots) of AR, LN-ST, LN-ST-S, HN-ST and HN-ST-S specimens are shown in Fig. 5a-d. During the forward and backward scans, the peak activation current (I_a) and peak reactivation current (I_r) were measured. In the forward scan, both the matrix and the Cr + Mo depleted regions next to the grain boundaries undergo dissolution giving rise to I_a. In the sensitised condition lack of sufficient Cr caused by intergranular precipitation of chromium-rich carbides results formation of weak and discontinuous passive film at the regions adjacent to the grain boundaries. During the reverse scan, these regions reactivate before the reactivation of bulk microstructure, which leads to higher I_r currents. With increasing annealing temperature I_r value increases from 1.02×10^{-4} to 0.0012 mA/cm^2 in LN-ST and from 7.84×10^{-6} to 3×10^{-6} mA/cm^2 in HN-ST, as shown in Fig. 5a and c. The value of I_r is more for LN-ST specimens as compared to HN-ST specimens. In the sensitised condition (Fig. 5b & d), I_r value tends to approach to I_a value. I_r values for LN-ST-S specimens have been found to be higher (0.0025 to 0.0113 mA/cm^2) as compared to that of HN-ST-S specimens (4.38×10^{-4} to 0.00106 mA/cm^2). Increased DOS values (Fig. 6) in sensitised condition indicate the

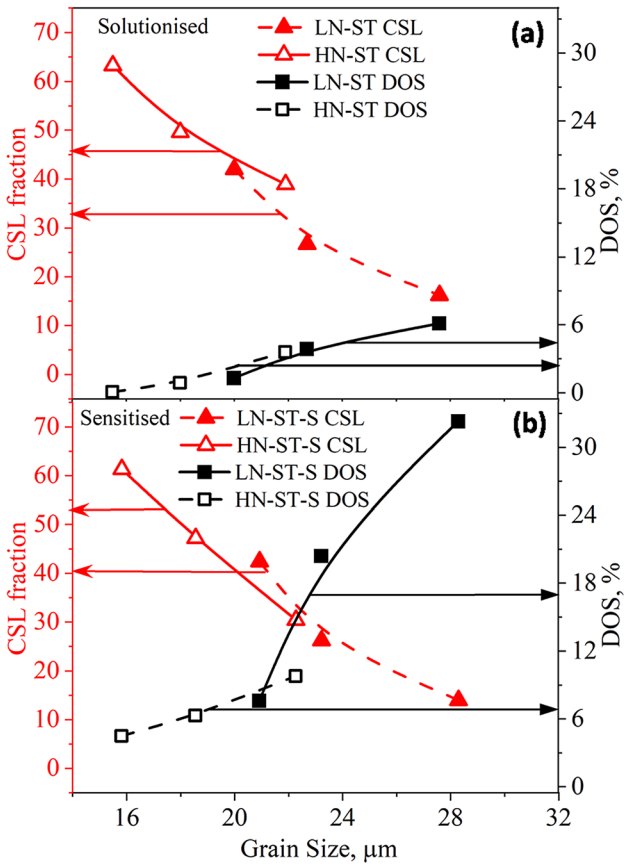

Fig. 6 Influence of GS on CSL and DOS for: **a** solutionised and **b** sensitised specimens

severity of IGC in LN-ST-S. It also indicates anodic dissolution to a greater extent. DOS value more than 5% in a DL-EPR test indicates medium to strong susceptibility to IGC [31]. Higher DOS value in all the sensitised specimens (in both the steels) suggests that steels are prone to IGC. These values are higher for LN-ST and LN-ST-S as compared to HN-ST and HN-ST-S specimens. It is worth noting that DOS value of as-received low nitrogen containing ASS in sensitised condition is 15, which is higher than 7 observed in as-received high nitrogen containing ASS. DOS value of both steels, LN-ST-S and HN-ST-S in 1000 °C annealed condition is the lowest which indicates improvement of IGC resistance of both steels after heat treatment. But it deteriorates with increasing annealing temperature. However, solutionised specimens recorded a lower DOS indicates that they are less prone to IGC.

3.3 Structure Property Correlation

From the foregoing sections it is evident that GS and SD of GS in both steels is accompanied by increase in FWHM with increasing solutionising temperature. Lower DOS is expected in solutionised condition with increasing solutionising temperatures; however, with increasing solutionising temperature, DOS value increases unusually (Fig. 6). Upon sensitisation, DOS value increases further. Higher DOS in LN-ST-S specimen as compared to other conditions indicates high susceptibility to sensitisation. Higher nitrogen in HN-ST-S reduces DOS significantly indicating the beneficial role of high nitrogen in ASS. Nitrogen

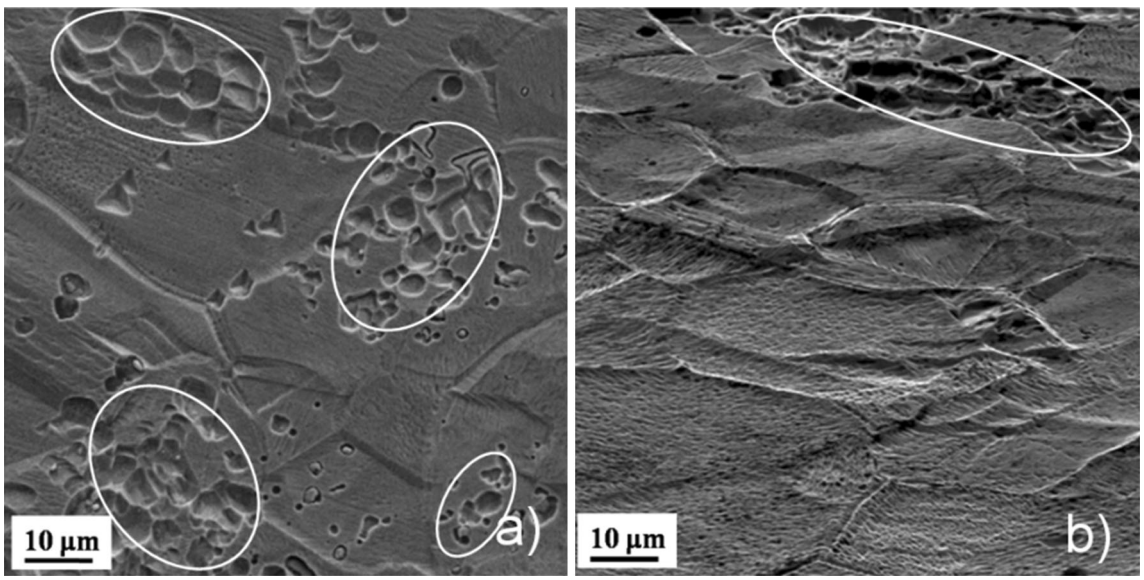

Fig. 7 Secondary electron images of corroded specimens solutionised at 1100 °C followed by sensitisation treatment at 675 °C: **a** showing corrosion pits (white elliptical regions) in low nitrogen steel, whereas high nitrogen steel shows **b** very few post corrosion pits

favours the formation of low energy Σ boundaries during annealing, by lowering the stacking fault energy. Low energy Σ boundaries improve corrosion resistance of materials [9, 11].

In order to establish structure property correlation between GS, CSL and DOS, both CSL and DOS were also plotted against GS, as shown in Fig. 6. It is apparent that DOS value increases with decreasing CSL fraction and increasing GS in solutionised condition. But, it is pronounced in sensitised condition, as shown in Fig. 6b. This is possibly due to the precipitation of $M_{23}C_6$ carbide at the grain boundaries [10, 11], which results weaker passive films causing higher anodic dissolution at the boundaries during corrosion test. The secondary electron images of corroded specimens (Fig. 7a and b) reveal the pronounced pitting in LN-ST-S specimen as compared to HN-ST-S specimen. It is worth noting that the attack at the grain boundaries is not severe in the present investigation due to absence of $M_{23}C_6$ precipitates. But, pittings are seen at some regions within the grains, as shown in Fig. 7a and b.

It is generally expected that the grain boundary area decreases with increased annealing temperature and improves the corrosion resistance of material. With increasing GS, total grain boundary area may be decreasing in the present case too, but the corrosion resistance does not increase. Though the high nitrogen containing ASS has smaller GS compared to low nitrogen containing ASS, it has higher fraction of low energy Σ boundaries. Hence, high nitrogen containing ASS exhibits better corrosion resistance. In the present study, passive film of corrosion tested specimens was not studied but extensive results are available in the literature [9, 32]. It has been reported that Mn, Cr, Mo and N additions in stainless steel improve dynamic nature of passive films and like Mo, N also forms concentration gradient in the passive films [9, 32]. Nitrogen can provide stability to passive film which improves corrosion resistance of steel. It is apparent that DOS values of LN-ST-S and HN-ST-S specimens are higher as compared to their respective as-received steels. The DOS value is 15.8 for low nitrogen containing ASS and 7.1 for high nitrogen containing ASS. Therefore, higher DOS for low nitrogen containing ASS could be due to reduced low energy Σ boundaries and weak passive film with increasing GS.

4 Conclusions

Influences of GS and SD of GS on corrosion resistance of low and high nitrogen containing ASS were studied in solutionised and sensitised conditions. Following conclusions have been drawn:

1. Grain size increased with increasing solutionising temperature accompanied by increased SD of grain size. Grain size was smaller in high nitrogen containing ASS as compared to low nitrogen containing ASS.
2. FWHM increased with increasing solutionising temperature but the values were higher in high nitrogen containing ASS.
3. High nitrogen containing ASS had higher fraction of low energy Σ boundaries in both solutionised and sensitised conditions as compared to low nitrogen ASS.
4. High nitrogen containing ASS exhibited better corrosion resistance even though it had finer grains and high FWHM. This was attributed to the higher fraction of low energy Σ boundaries resulted due to reduced stacking fault energy by nitrogen. On the other hand, low nitrogen containing ASS encountered severe IGC due to large scatter in grains size (i.e. SD) and reduced fraction of low energy boundaries.

Acknowledgements Authors acknowledge DST-FIST (Govt. of India) for FESEM facility and SERB (Govt. of India) for TSL-OIM software (Ref: CRG/2020/003968/MMM).

References

1. Taiwade RV, Shukla R, Vashishtha H, Ingle A V &Dayal RK, Effect of grain size on degree of sensitization of chrome-manganese stainless steel, *ISIJ Int.*, 53 (2013) 2206. https://doi.org/10.2355/isijinternational.53.2206
2. Kaithwas CK, Bhuyan P, Pradhan SK & Mandal S, Hall-Petch type of relationship between the extent of intergranular corrosion and grain size in a Ni-based superalloy, *Corros. Sci.*, 175 (2020) 108868, 14pp. https://doi.org/10.1016/j.corsci.2020.108868
3. Parvathavarthini N, Mulki S, Dayal RK, Samajdar I… & Raj B, Sensitization control in AISI 316L (N) austenitic stainless steel: Defining the role of the nature of grain boundary, *Corros. Sci.*, 51 (2009) 2144. https://doi.org/10.1016/j.corsci.2009.05.045
4. Hall EO, The deformation and ageing of mild steel: III discussion of results, *Proceedings of the Physical Society, Section B*, 64 (1951) 747.
5. Petch NJ, The cleavage strength of polycrystals, *J. Iron Steel Inst.*, 174 (1953) 25.
6. Abraham ST, Shivaprasad S, Das CR, Albert SK… &Balasubramaniam K, Characterisation of heterogeneous microstructure in large forged products using nonlinear ultrasonic method, *Mater. Sci. Technol..*, 36 (2020) 699. https://doi.org/10.1080/02670836.2020.1732077
7. Abraham ST, Albert SK, Das CR, Parvathavarthini N … &Balasubramaniam K, Assessment of sensitization in AISI 304 stainless steel by nonlinear ultrasonic method, *Acta Metall. Sin. - Engl*, 26 (2013) 545. https://doi.org/10.1007/s40195-013-0168-y
8. DayalRK, Parvathavarthini N, RajB, A review on the influence of metallurgical variables on the sensitization kinetics of austenitic stainlesssteels, *Int. Mater. Rev*. 50 (2005) 129. https://doi.org/10.1179/174328005X14348
9. Grabke HJ, The role of nitrogen in the corrosion of iron and steels, *ISIJ Int*., 36 (1996) 777

10. Poonguzhali A, Pujar MG &Kamachi MU, Effect of nitrogen and sensitization on the microstructure and pitting corrosion behavior of AISI type 316LN stainless steels, *J. Mater. Eng. Perform.*, 22 (2013) 1170. https://doi.org/10.1007/s11665-012-0356-3
11. Toppo A, Shankar V, George RP & Philip J, Effect of nitrogen on the intergranular stress corrosion cracking resistance of 316LN stainless steel, *Corrosion*, 76 (2020) 591. https://doi.org/10.5006/3417
12. Bain EC, Aborn RH & Rutherford JJB, The nature and prevention of intergranular corrosion in austenitic stainless steels, Trans. AmerSoc Steel Treating, 21 (1933) 481.
13. Tsurekawa S, Nakamichi S & Watanabe T, Correlation of grain boundary connectivity with grain boundary character distribution in austenitic stainless steel, *Acta Mater.*, 54 (2006) 3617-3626. https://doi.org/10.1016/j.actamat.2006.03.048
14. Michiuchi M, Kokawa H, Wang ZJ, Sato YS and Sakai K,Twin-induced grain boundary engineering for 316 austenitic stainless steel,*Acta Mater.,* 54 (2006) 5179. https://doi.org/10.1016/j.actamat.2006.06.030
15. Randle V, Grain boundary engineering: an overview after 25 years, *Mater. Sci. Technol.*, 26 (2010) 253. https://doi.org/10.1179/026708309X12601952777747
16. Schino A Di & Kenny J, Effect of grain size on the corrosion resistance of a high nitrogen-low nickel austenitic stainless steel, *J. Mater. Sci. Lett.*, 21(2002), 1969. https://doi.org/10.1023/A:1021625117639
17. Ganesan V, Laha K, Parameswaran P, Nandagopal M & Mathew MD, Effect of nitrogen on tensile flow behaviour of type 316 LN austenitic stainless steel, *Mater. High Temp.*, 32 (2015) 438. https://doi.org/10.1179/1878641314Y.0000000035
18. Momeni M, Moayed MH, &Davoodi A. Tuning DOS measuring parameters based on double-loop EPR in H2SO4 containing KSCN by Taguchi method, *Corros. Sci*., 52(2010) 2653. https://doi.org/10.1016/j.corsci.2010.04.015
19. Sinha P, Chakravarty S, Singh R, & Singh PK, Magnetization study of the sensitization in SS304LN, *Mater. Res. Bull.*, 109 (2019) 149
20. Majidi AP &Streicher MA, The double loop reactivation method for detecting sensitization in AISI 304 stainless steels, *Corrosion*, 40(1984) 584. https://doi.org/10.5006/1.3581921
21. Umemura F, Akashi M & Kawamoto T, Evaluation of IGSCC susceptibility of austenitic stainless steels using electrochemical reactivation method. *Corros. Eng*.., 29 (1980) 163. https://doi.org/10.3323/jcorr1974.29.4_163
22. Brandon DG, The structure of high-angle grain boundaries, *Acta Metall*., 14 (1966) 1479. https://doi.org/10.1016/0001-6160(66)90168-4
23. Yakubtsov IA, Ariapour A &Perovic DD, Effect of nitrogen on stacking fault energy of fcc iron-based alloys, *Acta Mater.*, 47(1999)1271. https://doi.org/10.1016/S1359-6454(98)00419-4
24. Jiang B, Qi X, Zhou W, Xi ZL & Hsu TY, The effect of nitrogen on shape memory effect in Fe-Mn-Si alloys, *Scr. Mater*.., 34 (1996)1437. https://doi.org/10.1016/1359-6462(95)00673-7
25. Schramm, RE & Reed RP, Stacking fault energies of seven commercial austenitic stainless steels, *Met. Trans. A*6 (1975) 1345. https://doi.org/10.1007/BF02641927
26. Stoltz RE, Vander Sande JB, The effect of nitrogen on stacking fault energy of Fe-Ni-Cr-Mn steels, *Met. Trans. A*, 11 (1980) 1033. https://doi.org/10.1007/BF02654717
27. Aamani S, Das CR, Martha SK and Panigrahi BB, Effect of nitrogen on grain boundary character distribution in 316 stainless steel, *Mater. Lett.*, 288 (2021) 129387. https://doi.org/10.1016/j.matlet.2021.129387
28. Mandal S, Bhaduri AK, &Sarma VS, Studies on twinning and grain boundary character distribution during anomalous grain growth in a Ti-modified austenitic stainless steel, *Mater. Sci. Eng. A*, 515 (2009) 134. https://doi.org/10.1016/j.msea.2009.02.042
29. Horton D, Thomson CB & Randle V, Aspects of twinning and grain growth in high purity and commercially pure nickel, *Mater. Sci. Eng. A*, 203 (1995) 408. https://doi.org/10.1016/0921-5093(95)09821-6
30. Randle V, Mechanism of twining-induced grain boundary engineering in low stacking-fault energy materials, *Acta Mater*., 47 (1999) 4187. https://doi.org/10.1016/S1359-6454(99)00277-3
31. International Standards Organization, Technical Committee 156:Corrosion of Metals and Alloys, Working Group 9: Corrosion Testing of Materials for Power Generation, "Revised Committee Draft ISO/CD 12372 for a Proposed Standard on Method for Electrochemical Potentiokinetic Reactivation Test," 7th Rev. version (Geneva, Switzerland: ISO, 1998).
32. Olsson CO &Landolt D, Passive films on stainless steels—chemistry, structure and growth, *Electrochim. Acta*, 48 (2003) 1093. https://doi.org/10.1016/S0013-4686(02)00841-1